CHAPTER

3

Kinematics

OUTLINE

CHAPTER OBJECTIVES

- To review the basic Cartesian and curvilinear coordinates systems
- To link fluid flow kinematics with the particle kinematics
- To define the various flow lines in unsteady fluid velocity fields
- To present fluid acceleration in the Eulerian flow-field formulation
- To establish the fundamental meaning of the strain rate and rotation tensors
- To present the means for time differentiating general three-dimensional volume integrations

3.1. INTRODUCTION AND COORDINATE SYSTEMS

Kinematics is the study of motion without reference to the forces or stresses that produce the motion. In this chapter, fluid kinematics is presented in two and three dimensions starting with simple fluid-particle-path concepts and then proceeding to topics of greater complexity.

These include: particle- and field-based descriptions for the time-dependent position, velocity, and acceleration of fluid particles; the relationship between the fluid velocity gradient tensor and the deformation and rotation of fluid elements; and the general mathematical relationships that govern arbitrary volumes that move and deform within flow fields. The forces and stresses that cause fluid motion are considered in subsequent chapters covering the *dynamics* or *kinetics* of the fluid motion.

In general, three independent spatial dimensions and time are needed to fully describe fluid motion. When a flow does not depend on time, it is called *steady*; when it does depend on time it is called *unsteady*. In addition, fluid motion is studied in fewer than three dimensions whenever possible because the necessary analysis is usually simpler and relevant phenomena are more easily understood and visualized.

A truly *one-dimensional flow* is one in which the flow's characteristics can be entirely described with one independent spatial variable. Few real flows are strictly one dimensional, although flows in long, straight constant-cross-section conduits come close. Here, the independent coordinate may be aligned with the flow direction, as in the case of low-frequency pulsations in a pipe as shown in Figure 3.1a, where z is the independent coordinate and darker gray indicates higher gas density. Alternatively, the independent coordinate may be aligned in the cross-stream direction, as in the case of viscous flow in a round tube where the radial distance, R, from the tube's centerline is the independent coordinate (Figure 3.1b). In addition, higher dimensional flows are sometimes analyzed in one dimension by averaging the properties of the higher dimensional flow over an appropriate distance or area (Figure 3.1c and d).

A *two-dimensional*, or *plane*, flow is one in which the variation of flow characteristics can be described by two spatial coordinates. The flow of an ideal fluid past a circular cylinder of infinite length having its axis perpendicular to the primary flow direction is an example of a plane flow (see Figure 3.2a). (Here we should note that the word *cylinder* may also be used in this context for any body having a cross-sectional shape that is invariant along its length even if this shape is not circular.) This definition of two-dimensional flow officially includes the flow around bodies of revolution where flow characteristics are identical in any plane that contains the body's axis (see Figure 6.27). However, such flows are customarily called *three-dimensional axisymmetric flows.*

A *three-dimensional* flow is one that can only be properly described with three independent spatial coordinates and is the most general case considered in this text. Sometimes curvilinear coordinates that match flow-field boundaries or symmetries simplify the analysis and description of flow fields. Thus, several different coordinate systems are used in this text (see Figure 3.3). Two-dimensional (plane) Cartesian and polar coordinates for an arbitrary point P (Figure 3.3a) may be denoted by the coordinate pairs (x, y), (x_1, x_2), or (r, θ) with the corresponding velocity components (u, v), (u_1, u_2), or (u_r, u_θ). In three dimensions, Cartesian coordinates (Figures 2.1 and 3.3b) may be used to locate a point P via the coordinate triplets (x, y, z) or (x_1, x_2, x_3) with corresponding velocity components (u, v, w) or (u_1, u_2, u_3). Cylindrical polar coordinates for P (Figure 3.3c) are denoted by (R, φ, z) with corresponding velocity components (u_R, u_φ, u_z). In addition, they will occasionally be denoted (r, θ, z) or (r, θ, x). Spherical polar coordinates for P (Figure 3.3d) are denoted by (r, θ, φ) with the corresponding velocity components $(u_r, u_\theta, u_\varphi)$. In all cases, unit vectors are denoted by **e** with an appropriate

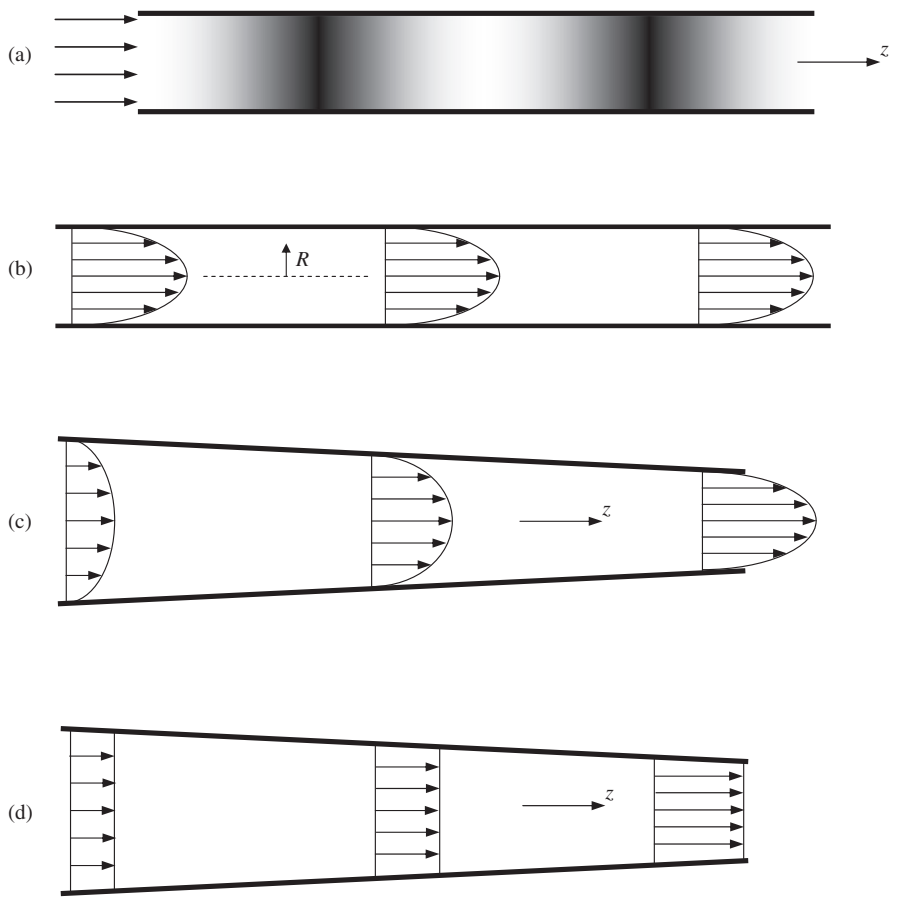

FIGURE 3.1 (a) Example of a one-dimensional fluid flow in which the gas density, shown by the grayscale, varies in the stream-wise z direction but not in the cross-stream direction. (b) Example of a one-dimensional fluid flow in which the fluid velocity varies in the cross-stream R direction but not in the stream-wise direction. (c) Example of a two-dimensional fluid flow where the fluid velocity varies in the cross-stream and stream-wise directions. (d) The one-dimensional approximation to the flow show in part (c). Here the approximate flow field varies only in the stream-wise z direction.

subscript as in (2.1) and Figure 2.1. More information about these coordinate systems is provided in Appendix B.

3.2. PARTICLE AND FIELD DESCRIPTIONS OF FLUID MOTION

There are two ways to describe fluid motion. In the *Lagrangian* description, fluid particles are followed as they move through a flow field. In the *Eulerian* description, a flow field's characteristics are monitored at fixed locations or in stationary regions of space. In fluid

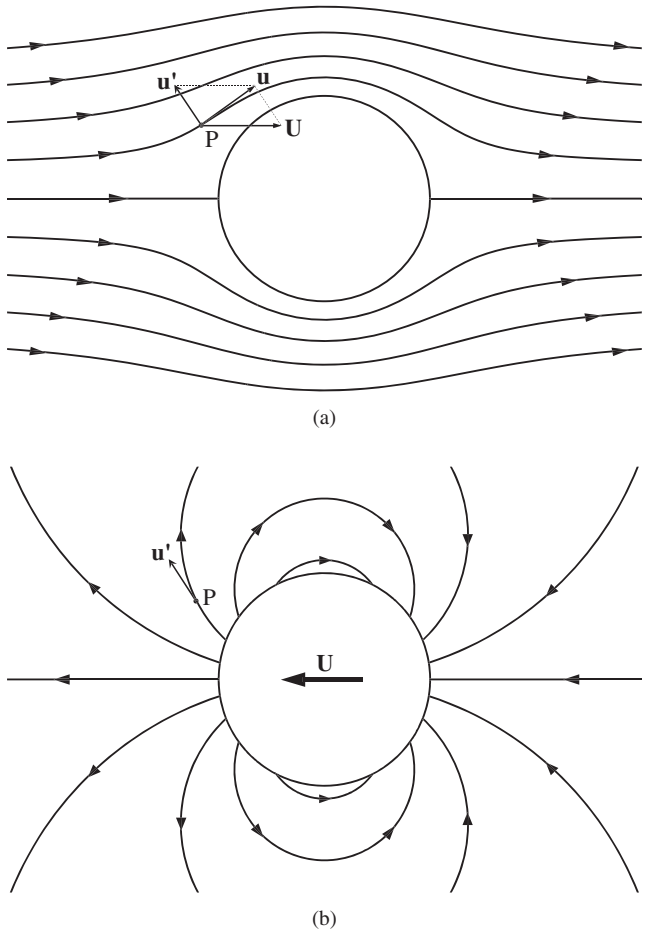

FIGURE 3.2 Sample flow fields where two spatial coordinates are needed. (a) Steady flow of an ideal incompressible fluid past a long stationary circular cylinder with its axis perpendicular to the flow. Here the total fluid velocity **u** at point P can be considered a sum of the flow velocity far from the cylinder **U**, and a velocity component **u**′ caused by the presence of the cylinder. (b) Unsteady flow of a nominally quiescent ideal incompressible fluid around a moving long circular cylinder with its axis perpendicular to the page. Here the cylinder velocity **U** is shown inside the cylinder, and the fluid velocity **u**′ at point P is caused by the presence of the moving cylinder alone. Although the two fields look very different, they only differ by a Galilean transformation. The streamlines in (a) can be changed to those in (b) by switching to a frame of reference where the fluid far from the cylinder is motionless.

mechanics, an understanding of both descriptions is necessary because the acceleration following a fluid particle is needed for the application of Newton's second law to fluid motion while observations, measurements, and simulations of fluid flows are commonly made at fixed locations or in stationary spatial regions with the fluid moving past the locations or through the regions of interest.

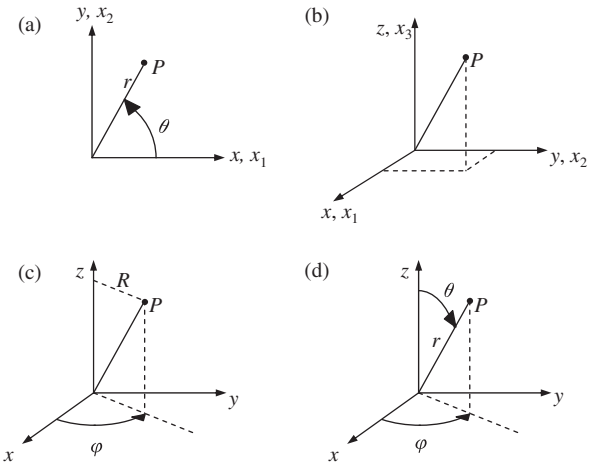

FIGURE 3.3 Coordinate systems commonly used in this text. In each case P is an arbitrary point away from the origin. (a) Plane Cartesian or polar coordinates where P is located by the coordinate pairs (x, y), (x_1, x_2), or (r, θ). (b) Three-dimensional Cartesian coordinates where P is located by the coordinate triplets (x, y, z) or (x_1, x_2, x_3). (c) Cylindrical polar coordinates where P is located by the coordinate triplet (R, φ, z). (d) Spherical polar coordinates where P is located by the coordinate triplet (r, θ, φ).

The Lagrangian description is based on the motion of fluid particles. It is the direct extension of single particle kinematics (e.g., see Meriam & Kraige, 2007) to a whole field of fluid particles that are labeled by their location, $\mathbf{r}_o$, at a reference time, $t = t_o$. The subsequent position $\mathbf{r}$ of each fluid particle as a function of time, $\mathbf{r}(t;\mathbf{r}_o,t_o)$, specifies the flow field. Here, $\mathbf{r}_o$ and t_o are boundary or initial condition parameters that label fluid particles, and are not independent variables. Thus, the current velocity $\mathbf{u}$ and acceleration $\mathbf{a}$ of the fluid particle that was located at $\mathbf{r}_o$ at time t_o are obtained from the first and second temporal derivatives of particle position $\mathbf{r}(t;\mathbf{r}_o,t_o)$:

$$\mathbf{u} = d\mathbf{r}(t;\mathbf{r}_o,t_o)/dt \quad \text{and} \quad \mathbf{a} = d^2\mathbf{r}(t;\mathbf{r}_o,t_o)/dt^2. \tag{3.1}$$

These values for $\mathbf{u}$ and $\mathbf{a}$ are valid for the fluid particle as it moves along its trajectory through the flow field (Figure 3.4). In this particle-based Lagrangian description of fluid motion, fluid particle kinematics are identical to that in ordinary particle mechanics, and any scalar, vector,

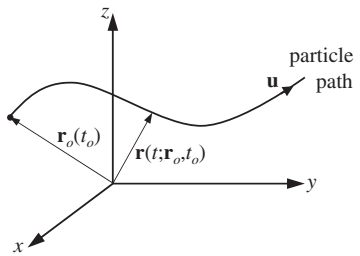

FIGURE 3.4 Lagrangian description of the motion of a fluid particle that started at location $\mathbf{r}_o$ at time t_o. The particle path or particle trajectory $\mathbf{r}(t;\mathbf{r}_o,t_o)$ specifies the location of the fluid particle at later times.

or tensor flow-field property F may depend on the path(s) followed of the relevant fluid particle(s) and time: $F = F[\mathbf{r}(t;\mathbf{r}_o,t_o), t]$.

The Eulerian description focuses on flow field properties at locations or in regions of interest, and involves four independent variables: the three spatial coordinates represented by the position vector $\mathbf{x}$, and time t. Thus, in this field-based Eulerian description of fluid motion, a flow-field property F depends directly on $\mathbf{x}$ and t: $F = F(\mathbf{x}, t)$. Even though this description complicates the calculation of $\mathbf{a}$, because individual fluid particles are not followed, it is the favored description of fluid motion.

Kinematic relationships between the two descriptions can be determined by requiring equality of flow-field properties when $\mathbf{r}$ and $\mathbf{x}$ define the same point in space, both are resolved in the same coordinate system, and a common clock is used to determine the time t:

$$F[\mathbf{r}(t;\mathbf{r}_o,t_o),t] = F(\mathbf{x},t) \quad \text{when} \quad \mathbf{x} = \mathbf{r}(t;\mathbf{r}_o,t_o). \tag{3.2}$$

Here the second equation specifies the trajectory followed by a fluid particle. This compatibility requirement forms the basis for determining and interpreting time derivatives in the Eulerian description of fluid motion. Applying a total time derivative to the first equation in (3.2) produces

$$\frac{d}{dt}F[\mathbf{r}(t;\mathbf{r}_o,t_o),t] = \frac{\partial F}{\partial r_1}\frac{dr_1}{dt} + \frac{\partial F}{\partial r_2}\frac{dr_2}{dt} + \frac{\partial F}{\partial r_3}\frac{dr_3}{dt} + \frac{\partial F}{\partial t} = \frac{d}{dt}F(\mathbf{x},t) \quad \text{when} \quad \mathbf{x} = \mathbf{r}(t;\mathbf{r}_o,t_o), \tag{3.3}$$

where the components of $\mathbf{r}$ are r_i. In (3.3), the time derivatives of r_i are the components u_i of the fluid particle's velocity $\mathbf{u}$ from (3.1). In addition, $\partial F/\partial r_i = \partial F/\partial x_i$ when $\mathbf{x} = \mathbf{r}$, so (3.3) becomes

$$\frac{d}{dt}F[\mathbf{r}(t;\mathbf{r}_o,t_o),t] = \frac{\partial F}{\partial x_1}u_1 + \frac{\partial F}{\partial x_2}u_2 + \frac{\partial F}{\partial x_3}u_3 + \frac{\partial F}{\partial t} = (\nabla F)\cdot\mathbf{u} + \frac{\partial F}{\partial t} \equiv \frac{D}{Dt}F(\mathbf{x},t), \tag{3.4}$$

where the final equality defines D/Dt as the total time derivative in the Eulerian description of fluid motion. It is the equivalent of the total time derivative d/dt in the Lagrangian description and is known as the *material derivative*, *substantial derivative*, or *particle derivative*, where the final attribution emphasizes the fact that it provides time derivative information following a fluid particle.

The material derivative D/Dt defined in (3.4) is composed of unsteady and advective acceleration terms. (1) The *unsteady* part of DF/Dt, $\partial F/\partial t$, is the *local* temporal rate of change of F at the location $\mathbf{x}$. It is zero when F is independent of time. (2) The *advective* (or *convective*) part of DF/Dt, $\mathbf{u}\cdot\nabla F$, is the rate of change of F that occurs as fluid particles move from one location to another. It is zero where F is spatially uniform, the fluid is not moving, or $\mathbf{u}$ and ∇F are perpendicular. For clarity and consistency in this book, the movement of fluid particles from place to place is referred to as *advection* with the term *convection* being reserved for the special circumstance of heat transport by fluid movement. In vector and index notations, (3.4) is commonly rearranged slightly and written as

$$\frac{DF}{Dt} \equiv \frac{\partial F}{\partial t} + \mathbf{u}\cdot\nabla F, \quad \text{or} \quad \frac{DF}{Dt} \equiv \frac{\partial F}{\partial t} + u_i\frac{\partial F}{\partial x_i}. \tag{3.5}$$

The scalar product $\mathbf{u} \cdot \nabla F$ is the magnitude of $\mathbf{u}$ times the component of ∇F in the direction of $\mathbf{u}$ so (3.5) can then be written in scalar notation as

$$\frac{DF}{Dt} \equiv \frac{\partial F}{\partial t} + |\mathbf{u}| \frac{\partial}{\partial s}, \tag{3.6}$$

where s is a path-length coordinate on the fluid particle trajectory $\mathbf{x} = \mathbf{r}(t;\mathbf{r}_o,t_o)$, that is, $d\mathbf{r} = \mathbf{e}_\mathbf{u} ds$ with $\mathbf{e}_\mathbf{u} = \mathbf{u}/|\mathbf{u}|$.

3.3. FLOW LINES, FLUID ACCELERATION, AND GALILEAN TRANSFORMATION

In the Eulerian description, three types of curves are commonly used to describe fluid motion—streamlines, path lines, and streak lines. These are defined and described here assuming that the fluid velocity vector, $\mathbf{u}$, is known at every point of space and instant of time throughout the region of interest. Streamlines, path lines, and streak lines all coincide when the flow is steady. These curves are often valuable for understanding fluid motion and form the basis for experimental techniques that track seed particles or dye filaments. Pictorial and photographic examples of flow lines can be found in specialty volumes devoted to flow visualization (Van Dyke, 1982; Samimy et al., 2003).

A *streamline* is a curve that is instantaneously tangent to the fluid velocity throughout the flow field. In unsteady flows the streamline pattern changes with time. In Cartesian coordinates, if $d\mathbf{s} = (dx, dy, dz)$ is an element of arc length along a streamline (Figure 3.5) and $\mathbf{u} = (u, v, w)$ is the local fluid velocity vector, then the tangency requirement on $d\mathbf{s}$ and $\mathbf{u}$ leads to

$$dx/u = dy/v = dz/w \tag{3.7}$$

(see Exercise 3.3), and $\mathbf{u} \times d\mathbf{s} = 0$ because $d\mathbf{s}$ and $\mathbf{u}$ are locally parallel. Integrating (3.7) in both the upstream and downstream directions from a variety of reference locations allows streamlines to be determined throughout the flow field. If these reference

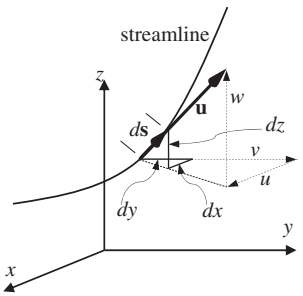

FIGURE 3.5 Streamline geometry. The arc-length element of a streamline, $d\mathbf{s}$, is locally tangent to the fluid velocity $\mathbf{u}$ so its components and the components of the velocity must follow (3.7).

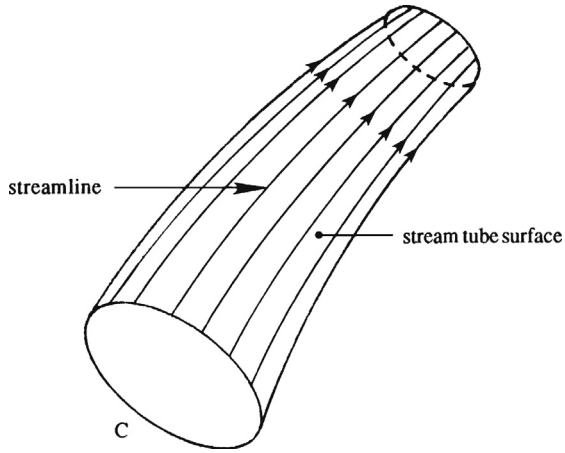

FIGURE 3.6 Stream tube geometry for the closed curve *C*.

locations lie on a closed curve *C*, the resulting stream surface is called a *stream tube* (Figure 3.6). No fluid crosses a stream tube's surface because the fluid velocity vector is everywhere tangent to it. Streamlines are useful in the depiction of flow fields and important for calculations involving simplifications (Bernoulli equations) of the full equations of fluid motion. In experiments, streamlines may be visualized by particle streak photography or by integrating (3.7) using measured velocity fields.

A *path line* is the trajectory of a fluid particle of fixed identity. It is defined in (3.2) and (3.3) as $\mathbf{x} = \mathbf{r}(t;\mathbf{r}_o,t_o)$. The equation of the path line for the fluid particle launched from $\mathbf{r}_o$ at t_o is obtained from the fluid velocity $\mathbf{u}$ by integrating

$$d\mathbf{r}/dt = [\mathbf{u}(\mathbf{x},t)]_{\mathbf{x}=\mathbf{r}} = \mathbf{u}(\mathbf{r},t) \tag{3.8}$$

subject to the requirement $\mathbf{r}(t_o) = \mathbf{r}_o$. Other path lines are obtained by integrating (3.8) from different values of $\mathbf{r}_o$ or t_o. A discretized version of (3.8) is the basis for particle image velocimetry (PIV), a popular and powerful flow field measurement technique (Raffel et al., 1998).

A *streak line* is the curve obtained by connecting all the fluid particles that will pass or have passed through a fixed point in space. The streak line through the point $\mathbf{x}_o$ at time t is found by integrating (3.8) for all relevant reference times, t_o, subject to the requirement $\mathbf{r}(t_o) = \mathbf{x}_o$. When completed, this integration provides a path line, $\mathbf{x} = \mathbf{r}(t;\mathbf{x}_o,t_o)$, for each value of t_o. At a fixed time t, the components of these path-line equations, $x_i = r_i(t;\mathbf{x}_o,t_o)$, provide a parametric specification of the streak line with t_o as the parameter. Alternatively, these path-line component equations can sometimes be combined to eliminate t_o and thereby produce an equation that directly specifies the streak line through the point $\mathbf{x}_o$ at time t. Streak lines may be visualized in experiments by injecting a passive marker, like dye or smoke, from a small port and observing were it goes as it is carried through the flow field by the moving fluid.

EXAMPLE 3.1

In two-dimensional Cartesian coordinates, determine the streamline, path line, and streak line that pass through the origin of coordinates at $t = t'$ in the unsteady near-surface flow field typical of long-wavelength water waves with amplitude ξ_o: $u = \omega\xi_o \cos(\omega t)$ and $v = \omega\xi_o \sin(\omega t)$.

Streamline Solution

Utilize the first equality in (3.7) to find:

$$\frac{dy}{dx} = \frac{v}{u} = \frac{\omega\xi_o \sin(\omega t')}{\omega\xi_o \cos(\omega t')} = \tan\Big(\omega t'\Big).$$

Integrating once produces: $y = x\tan(\omega t') + const$. For the streamline to pass through the origin ($x = y = 0$), the constant must equal zero, so the streamline equation is: $y = x\tan(\omega t')$.

Path-line Solution

Set $\mathbf{r} = [(x(t), y(t)]$, and use both components of (3.8) to find:

$$dx/dt = u = \omega\xi_o \cos(\omega t), \quad \text{and} \quad dy/dt = v = \omega\xi_o \sin(\omega t).$$

Integrate each of these equations once to find: $x = \xi_o \sin(\omega t) + x_o$, and $y = -\xi_o \cos(\omega t) + y_o$, where x_o and y_o are integration constants. The path-line requirement at $x = y = 0$ and $t = t'$ implies $x_o = -\xi_o \sin(\omega t')$, and $y_o = \xi_o \cos(\omega t')$, so the path-line component equations are:

$$x = \xi_o[\sin(\omega t) - \sin(\omega t')] \quad \text{and} \quad y = \xi_o[-\cos(\omega t) + \cos(\omega t')].$$

Here, the time variable t can be eliminated via a little algebra to find

$$\Big(x + \xi_o \sin(\omega t')\Big)^2 + \Big(y - \xi_o \cos(\omega t')\Big)^2 = \xi_o^2,$$

which is the equation of a circle of radius ξ_o centered on the location $[-\xi_o \sin(\omega t'), \xi_o \cos(\omega t')]$.

Streak-line Solution

To determine the streak line that passes through the origin of coordinates at $t = t'$, the location of the fluid particle that passed through $x = y = 0$ at $t = t_o$ must be found. Use the path-line results above but evaluate at t_o instead of t' to find different constants. Thus the parametric streak-line component equations are:

$$x = \xi_o[\sin(\omega t) - \sin(\omega t_o)] \quad \text{and} \quad y = \xi_o[-\cos(\omega t) + \cos(\omega t_o)].$$

Combine these equations to eliminate t_o and evaluate the result at $t = t'$ to find the required streak line:

$$\Big(x - \xi_o \sin(\omega t')\Big)^2 + \Big(y + \xi_o \cos(\omega t')\Big)^2 = \xi_o^2.$$

This is the equation of a circle of radius ξ_o centered on the location $[\xi_o \sin(\omega t'), -\xi_o \cos(\omega t')]$. The three flow lines in this example are shown in Figure 3.7. In this case, the streamline, path line, and streak line are all tangent to each other at the origin of coordinates.

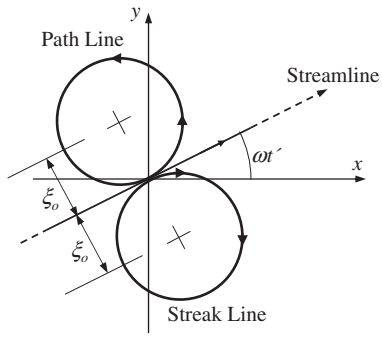

FIGURE 3.7 Streamline, path line, and streak line for Example 3.1. All three are distinct because the flow field is unsteady.

From this example it should be clear that streamlines, path lines, and streak lines differ in an unsteady flow field. This situation is also illustrated in Figure 3.2, which shows streamlines when there is relative motion of a circular cylinder and an ideal fluid. Figure 3.2a shows streamlines for a stationary cylinder with the fluid moving past it, a steady flow. Here, fluid particles that approach the cylinder are forced to move up or down to go around it. Figure 3.2b shows streamlines for a moving cylinder in a nominally quiescent fluid, an unsteady flow. Here, streamlines originate on the left side of the advancing cylinder where fluid particles are pushed to the left to make room for the cylinder. These streamlines curve backward and fluid particles move rightward at the cylinder's widest point. These streamlines terminate on the right side of the cylinder where fluid particles again move to the left to fill in the region behind the moving cylinder. Although their streamline patterns appear dissimilar, these flow fields only differ by a Galilean transformation. Consider the fluid velocity at a point P that lies at the same location relative to the cylinder in both fields. If $\mathbf{u}'$ is the fluid velocity at P in Figure 3.2b where the cylinder is moving at speed $\mathbf{U}$, then the fluid velocity $\mathbf{u}$ at P in Figure 3.2a is $\mathbf{u} = \mathbf{U} + \mathbf{u}'$. If $\mathbf{U}$ is constant, the fluid acceleration in both fields must be the same at the same location relative to the cylinder.

This expectation can be verified in general using (3.5) with F replaced by the fluid velocity observed in different coordinate frames. Consider a Cartesian coordinate system $O'x'y'z'$ that moves at a constant velocity $\mathbf{U}$ with respect to a stationary system $Oxyz$ having parallel axes (Figure 3.8). The fluid velocity $\mathbf{u}'(\mathbf{x}', t')$ observed in $O'x'y'z'$ will be related to the fluid velocity $\mathbf{u}(\mathbf{x},t)$ observed in $Oxyz$ by $\mathbf{u}(\mathbf{x},t) = \mathbf{U} + \mathbf{u}'(\mathbf{x}', t')$ when $t = t'$ and $\mathbf{x} = \mathbf{x}' + \mathbf{U}t + \mathbf{x}'_o$, where $\mathbf{x}'_o$ is the vector distance from O to O' at $t = 0$. Under these conditions it can be shown that

$$\frac{\partial \mathbf{u}}{\partial t} + (\mathbf{u} \cdot \nabla)\mathbf{u} = \left(\frac{D\mathbf{u}}{Dt}\right)_{in\ Oxyz} = \left(\frac{D\mathbf{u}'}{Dt'}\right)_{in\ O'x'y'z'} = \frac{\partial \mathbf{u}'}{\partial t'} + (\mathbf{u}' \cdot \nabla')\mathbf{u}' \tag{3.9}$$

(Exercise 3.12) where ∇' operates on the primed coordinates. The first and second terms of the leftmost part of (3.9) are the unsteady and advective acceleration terms in $Oxyz$. The unsteady acceleration term, $\partial \mathbf{u}/\partial t$, is nonzero at $\mathbf{x}$ when $\mathbf{u}$ varies with time at $\mathbf{x}$. It is zero everywhere when the flow is steady. The advective acceleration term, $(\mathbf{u} \cdot \nabla)\mathbf{u}$, is nonzero when fluid particles move between locations where the fluid velocity is different. It is zero when the fluid

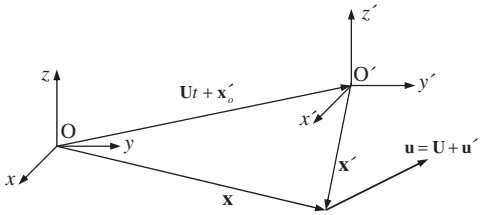

FIGURE 3.8 Geometry for showing that the fluid particle acceleration as determined by (3.9) is independent of the frame of reference when the frames differ by a Galilean transformation. Here Oxyz is stationary and O′$x'y'z'$ moves with respect to it at a constant speed **U**, the axes of the two frames are parallel, and **x** and **x**′ represent the same location. The fluid velocity observed at **x** in frame Oxyz is **u**. The fluid velocity observed at **x**′ in frame O′$x'y'z'$ is **u**′.

velocity is zero, the fluid velocity is uniform in space, or when the fluid velocity only varies in the cross-stream direction. In addition, the unsteady term is linear in **u** while the advective term is nonlinear (quadratic) in **u**. This nonlinearity is a primary feature of fluid mechanics. When **u** is small enough for this nonlinearity to be ignored, fluid mechanics reduces to acoustics or, when $\mathbf{u} = 0$, to fluid statics.

When examined together, the sample flow fields in Figure 3.2 and the Galilean invariance of the Eulerian fluid acceleration, (3.9), show that the relative importance of the steady and advective fluid-acceleration terms depends on the frame of reference of the observer. Figure 3.2a depicts a steady flow where the streamlines do not depend on time. Thus, the unsteady acceleration term, $\partial\mathbf{u}/\partial t$, is zero. However, the streamlines do bend in the vicinity of the cylinder so fluid particles must feel some acceleration because the absence of fluid-particle acceleration in a flow field corresponds to constant fluid-particle velocity and straight streamlines. Therefore, the advective acceleration term, $(\mathbf{u} \cdot \nabla)\mathbf{u}$, is nonzero for the flow in Figure 3.2a. In Figure 3.2b, the flow is unsteady and the streamlines are curved, so both acceleration terms in the rightmost part of (3.9) are nonzero. These observations imply that a Galilean transformation can alter the relative importance of the unsteady and advective fluid acceleration terms without changing the overall fluid-particle acceleration. Thus, an astutely chosen, steadily moving coordinate system can be used to enhance (or reduce) the relative importance of either the unsteady or advective fluid-acceleration term.

Additional insights into the character of the unsteady and advective acceleration terms might also be obtained from the reader's observations and experiences. For example, a nonzero unsteady acceleration is readily observed at any street intersection regulated by a traffic light with the moving or stationary vehicles taking the place of fluid particles. Here, a change in the traffic light may halt east-west vehicle flow and allow north-south vehicle flow to begin, thereby producing a time-dependent 90° rotation of the traffic-flow streamlines at the intersection location. Similarly, a nonzero advective acceleration is readily observed or experienced by roller-coaster riders when an analogy is made between the roller-coaster track and a streamline. While stationary and waiting in line, soon-to-be roller-coaster riders can observe that the track's shape involves hills, curves, and bends, and that this shape does not depend on time. This situation is analogous to the stationary observer of a nontrivial steady fluid flow—like that depicted in Figure 3.2a—who readily notes that streamlines curve and bend but do not depend

on time. Thus, the unsteady acceleration term is zero for both the roller coaster and a steady flow because both the roller-coaster cars and fluid particles travel through space on fixed-shape trajectories and achieve consistent (time-independent) velocities at any point along the track or streamline. However, anyone who has ever ridden a roller coaster will know that significant acceleration is possible while following a roller-coaster's fixed-shape track because a roller-coaster car's velocity varies as it traverses the track. These velocity variations result from the advective acceleration, and fluid particles that follow curved fixed-shape streamlines experience it as well. Within this roller coaster-streamline analogy a nonzero unsteady acceleration would correspond to roller-coaster cars and fluid particles following time-dependent paths. Such a possibility is certainly unusual for roller-coaster riders; roller-coaster tracks are nearly rigid, seldom fall down (thankfully), and are typically designed to produce consistent car velocities at each point along the track.

3.4. STRAIN AND ROTATION RATES

Given the definition of a fluid as a material that deforms continuously under the action of a shear stress, the basic constitutive law for fluids relates fluid element *deformation rates* to the stresses (surface forces per unit area) applied to a fluid element. This section describes fluid-element deformation and rotation rates in terms of the fluid *velocity gradient tensor*, $\partial u_i/\partial x_j$. The constitutive law for Newtonian fluids is covered in the next chapter. The various illustrations and interpretations provided here are analogous to their counterparts in solid mechanics when the fluid-appropriate *strain rate* (based on velocity $\mathbf{u}$) is replaced by the solid-appropriate *strain* (based on displacement $\mathbf{u}$).

The relative motion between two neighboring points can be written as the sum of the motion due to local rotation and deformation. Consider the situation depicted in Figure 3.9, and let $\mathbf{u}(\mathbf{x},t)$ be the velocity at point O (position vector $\mathbf{x}$), and let $\mathbf{u}+d\mathbf{u}$ be the velocity at the same time at a nearby neighboring point P (position vector $\mathbf{x}+d\mathbf{x}$). A three-dimensional first-order Taylor expansion of $\mathbf{u}$ about $\mathbf{x}$ leads to the following relationship between the components of $d\mathbf{u}$ and $d\mathbf{x}$:

$$du_i = (\partial u_i/\partial x_j)dx_j. \tag{3.10}$$

The term in parentheses in (3.10), $\partial u_i/\partial x_j$, is the velocity gradient tensor, and it can be decomposed into symmetric, S_{ij}, and antisymmetric, R_{ij}, tensors:

$$\frac{\partial u_i}{\partial x_j} = S_{ij} + \frac{1}{2}R_{ij}, \quad \text{where} \quad S_{ij} = \frac{1}{2}\left(\frac{\partial u_i}{\partial x_j} + \frac{\partial u_j}{\partial x_i}\right), \quad \text{and} \quad R_{ij} = \frac{\partial u_i}{\partial x_j} - \frac{\partial u_j}{\partial x_i}. \tag{3.11, 3.12, 3.13}$$

Here, S_{ij} is the *strain rate tensor*, and R_{ij} is the *rotation tensor*. The decomposition of $\partial u_i/\partial x_j$ provided by (3.11) is important when formulating the conservation equations for fluid motion because S_{ij}, which embodies fluid element deformation, is related to the stress field in a moving fluid while R_{ij}, which embodies fluid element rotation, is not.

The strain rate tensor has on- and off-diagonal terms. The diagonal terms of S_{ij} represent elongation and contraction per unit length in the various coordinate directions, and are sometimes called *linear* strain rates. A geometrical interpretation of S_{ij}'s first component, S_{11}, is

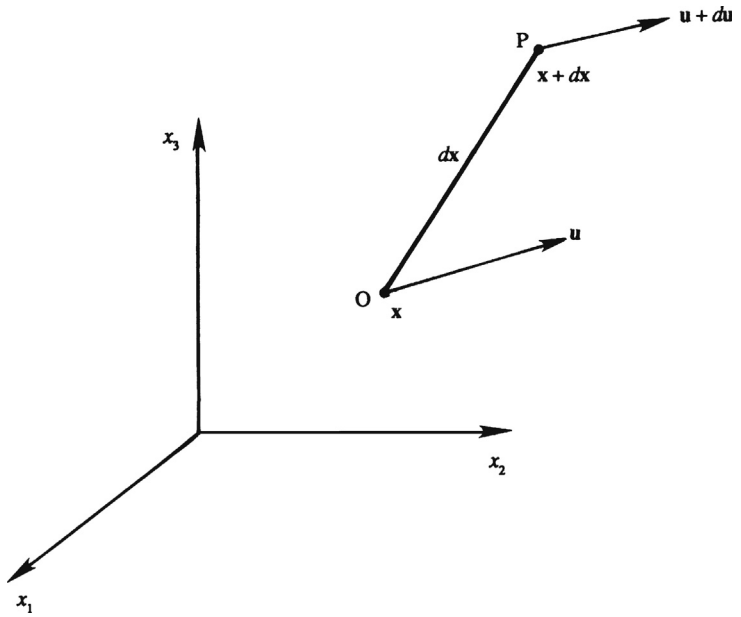

FIGURE 3.9 Velocity vectors $\mathbf{u}$ and $\mathbf{u} + d\mathbf{u}$ at two neighboring points O and P, respectively, that are separated by the short distance $d\mathbf{x}$.

provided in Figure 3.10. The rate of change of fluid element length in the x_1-direction per unit length in this direction is

$$\frac{1}{\delta x_1}\frac{D}{Dt}(\delta x_1) = \lim_{dt\to 0}\frac{1}{dt}\left(\frac{A'B' - AB}{AB}\right) = \lim_{dt\to 0}\frac{1}{\delta x_1 dt}\left(\delta x_1 + \frac{\partial u_1}{\partial x_1}\delta x_1 dt - \delta x_1\right) = \frac{\partial u_1}{\partial x_1},$$

where D/Dt indicates that the fluid element is followed as extension takes place. This simple construction is readily extended to the other two Cartesian directions, and in general the linear strain rate in the η direction is $\partial u_\eta/\partial x_\eta$ where *no summation* over the repeated η-index is implied. (Greek subscripts are commonly used when the summation convention is not followed.)

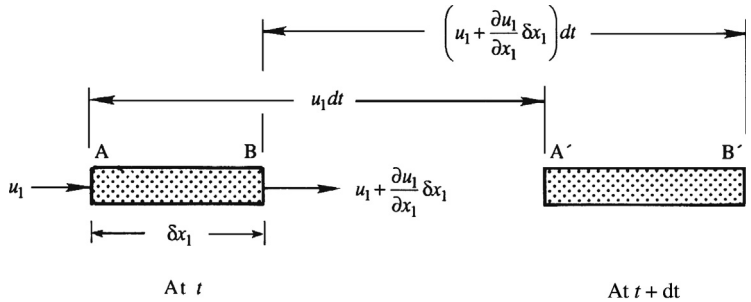

FIGURE 3.10 Illustration of positive linear strain rate in the first coordinate direction. Here $A'B' = AB + BB' - AA'$, and a positive $S_{11} = \partial u_1/\partial x_1$ corresponds to a lengthening of the fluid element.

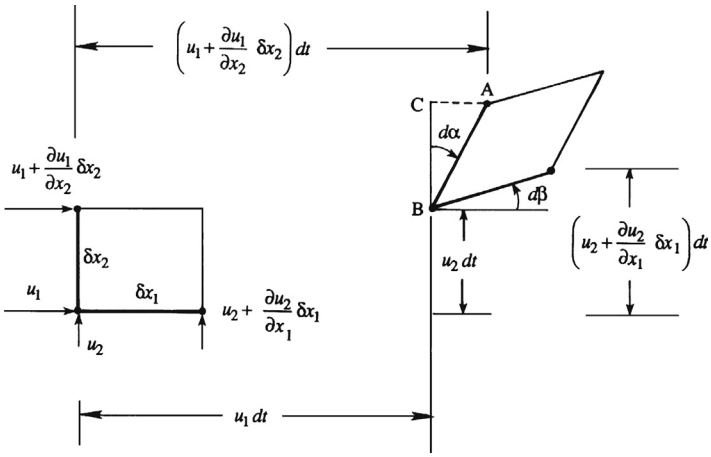

FIGURE 3.11 Illustration of positive deformation of a fluid element in the plane defined by the first and second coordinate directions. Here, both $\partial u_1/\partial x_2$ and $\partial u_2/\partial x_1$ are shown as positive, so $S_{12} = S_{21}$ from (3.12) is also positive. The deformation angle $d\alpha = \angle CBA$ is proportional to $\partial u_1/\partial x_2$ while $d\beta$ is proportional to $\partial u_2/\partial x_1$.

The off-diagonal terms of S_{ij} represent shear deformations that change the relative orientations of line segments initially parallel to the i- and j-directions in the flow. A geometrical interpretation of S_{ij}'s first off-diagonal component, $S_{12} = S_{21}$, is provided in Figure 3.11. The average rate at which the initially perpendicular segments δx_1 and δx_2 rotate toward each other is

$$\frac{1}{2}\frac{D(\alpha+\beta)}{Dt} = \lim_{dt\to 0}\frac{1}{2dt}\left(\frac{1}{\delta x_2}\left(\frac{\partial u_1}{\partial x_2}\delta x_2 dt\right)+\frac{1}{\delta x_1}\left(\frac{\partial u_2}{\partial x_1}\delta x_1 dt\right)\right) = \frac{1}{2}\left(\frac{\partial u_1}{\partial x_2}+\frac{\partial u_2}{\partial x_1}\right) = S_{12} = S_{21},$$

where again D/Dt indicates that the fluid element is followed as shear deformation takes place, and again this simple construction is readily extended to the other two Cartesian direction pairs. Thus, the off-diagonal terms of S_{ij} represent the average rate at which line segments initially parallel to the i- and j-directions rotate *toward* each other.

Here we also note that S_{ij} is zero for any rigid body motion composed of translation at a spatially uniform velocity $\mathbf{U}$ and rotation at a constant rate $\boldsymbol{\Omega}$ (see Exercise 3.17). Thus, S_{ij} is independent of the frame of reference in which it is observed, even if $\mathbf{U}$ depends on time and the frame of reference is rotating.

The first invariant of S_{ij} (the sum of its diagonal terms) is the *volumetric strain rate* or *bulk strain rate*. For a small volume $\delta V = \delta x_1 \delta x_2 \delta x_3$, it can be shown (Exercise 3.18) that

$$\frac{1}{\delta V}\frac{D}{Dt}(\delta V) = \frac{\partial u_1}{\partial x_1}+\frac{\partial u_2}{\partial x_2}+\frac{\partial u_3}{\partial x_3} = \frac{\partial u_i}{\partial x_i} = S_{ii}. \tag{3.14}$$

Thus, S_{ii} specifies the rate of volume change per unit volume and it does not depend on the orientation of the coordinate system.

The second member of the strain-rate decomposition (3.11) is the rotation tensor, R_{ij}. It is antisymmetric so its diagonal elements are zero and its off-diagonal elements are equal and opposite. Furthermore, its three independent elements can be put in correspondence with a vector. From (2.26), (2.27), or (3.13), this vector is the *vorticity*, $\boldsymbol{\omega} = \nabla \times \mathbf{u}$, and the correspondence is

$$R_{ij} = -\varepsilon_{ijk}(\nabla \times \mathbf{u})_k = -\varepsilon_{ijk}\omega_k = \begin{bmatrix} 0 & -\omega_3 & \omega_2 \\ \omega_3 & 0 & -\omega_1 \\ -\omega_2 & \omega_1 & 0 \end{bmatrix}, \qquad (2.26, 2.27, 3.15)$$

where

$$\omega_1 = \frac{\partial u_3}{\partial x_2} - \frac{\partial u_2}{\partial x_3}, \quad \omega_2 = \frac{\partial u_1}{\partial x_3} - \frac{\partial u_3}{\partial x_1}, \quad \text{and} \quad \omega_3 = \frac{\partial u_2}{\partial x_1} - \frac{\partial u_1}{\partial x_2}. \qquad (2.25, 3.16)$$

Figure 3.11 illustrates the motion of an initially square fluid element in the (x_1,x_2)-plane when $\partial u_1/\partial x_2$ and $\partial u_2/\partial x_1$ are nonzero and unequal so that $-\omega_3 = R_{12} = -R_{21} \neq 0$. In this situation, the fluid element translates and deforms in the (x_1,x_2)-plane, and rotates about the third coordinate axis. The average rotation rate is

$$\frac{1}{2}\frac{D(-\alpha+\beta)}{Dt} = \lim_{dt\to 0}\frac{1}{2dt}\left(-\frac{1}{\delta x_2}\left(\frac{\partial u_1}{\partial x_2}\delta x_2 dt\right) + \frac{1}{\delta x_1}\left(\frac{\partial u_2}{\partial x_1}\delta x_1 dt\right)\right) = \frac{1}{2}\left(-\frac{\partial u_1}{\partial x_2} + \frac{\partial u_2}{\partial x_1}\right)$$
$$= -\frac{R_{12}}{2} = \frac{R_{21}}{2},$$

where again D/Dt indicates that the fluid element is followed as rotation takes place, and again this simple construction is readily extended to the other two Cartesian direction pairs. Thus, $\boldsymbol{\omega}$ and R_{ij} represent twice the fluid element rotation rate (see also Exercise 2.1). This means that $\boldsymbol{\omega}$ and R_{ij} depend on the frame of reference in which they are determined since it is possible to choose a frame of reference that rotates with the fluid particle of interest at the time of interest. In such a co-rotating frame, $\boldsymbol{\omega}$ and R_{ij} will be zero but they will be nonzero if they are determined in a frame of reference that rotates at a different rate (see Exercise 3.19).

Interestingly, the presence or absence of fluid rotation often determines the character of a flow, and this dependence leads to two additional kinematic concepts related to fluid rotation. First, fluid motion is called *irrotational* if

$$\boldsymbol{\omega} = 0, \quad \text{or} \quad \text{equivalently} \quad R_{ij} = \partial u_i/\partial x_j - \partial u_j/\partial x_i = 0. \qquad (3.17)$$

When (3.17) is true, the fluid velocity $\mathbf{u}$ can be written as the gradient of a scalar function $\phi(\mathbf{x},t)$ because $u_i = \partial\phi/\partial x_i$ satisfies the condition of irrotationality (see Exercises 2.4 and 2.20). Although this may seem to be an unnecessary mathematical complication, finding a scalar function $\phi(\mathbf{x},t)$ such that $\nabla\phi$ solves the irrotational equations of fluid motion is sometimes easier than solving these equations directly for the vector velocity $\mathbf{u}(\mathbf{x},t)$ in the same circumstance.

The second concept related to fluid rotation is the extension of the vorticity, twice the fluid rotation rate at a point, to the *circulation* Γ, the amount of fluid rotation within a closed contour (or *circuit*) C. Here the circulation Γ is defined by

$$\Gamma \equiv \oint_C \mathbf{u}\cdot d\mathbf{s} = \int_A \boldsymbol{\omega}\cdot\mathbf{n}dA, \qquad (3.18)$$

where $d\mathbf{s}$ is an element of C, and the geometry is shown in Figure 3.12. The loop through the first integral sign signifies that C is a closed circuit and is often omitted. The second equality in (3.18) follows from Stokes' theorem (Section 2.13) and the definition of the vorticity

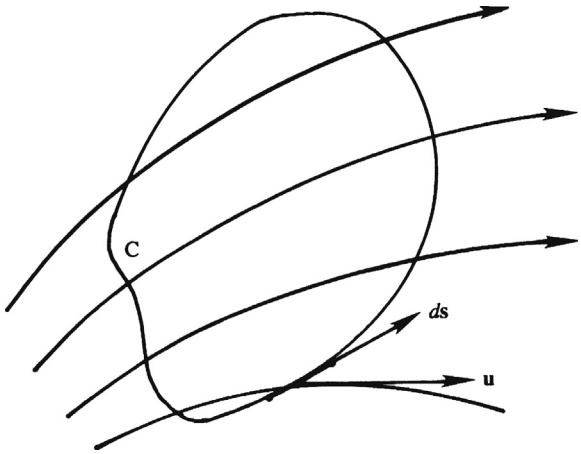

FIGURE 3.12 The circulation around the closed contour C is the line integral of the dot product of the velocity $\mathbf{u}$ and the contour element $d\mathbf{s}$.

$\boldsymbol{\omega} = \nabla \times \mathbf{u}$. The second equality requires the line integral of $\mathbf{u}$ around a closed curve C to be equal to the *flux of vorticity* through the arbitrary surface A bounded by C. Here, and elsewhere in this text, the term *flux* is used for the integral of a vector field normal to a surface. Equation (3.18) allows $\boldsymbol{\omega}$ to be identified as *the circulation per unit area.* This identification also follows directly from the definition of the curl as the limit of the circulation integral (see (2.35)).

Returning to the situation in Figure 3.9, equations (3.11) through (3.14) allow (3.10) to be rewritten as

$$du_i = \left(S_{ij} - \frac{1}{2}\varepsilon_{ijk}\omega_k \right) dx_j = S_{ij}dx_j + \frac{1}{2}(\boldsymbol{\omega} \times d\mathbf{x})_i, \tag{3.19}$$

where $\varepsilon_{ijk}\omega_k dx_j$ is the i-component of the cross product $-\boldsymbol{\omega} \times d\mathbf{x}$ (see (2.21)). Thus, the meaning of the second term in (3.19) can be deduced as follows. The velocity at a distance $\mathbf{x}$ from the axis of rotation of a rigid body rotating at angular velocity $\boldsymbol{\Omega}$ is $\boldsymbol{\Omega} \times \mathbf{x}$. The second term in (3.19) therefore represents the velocity of point P relative to point O because of an angular velocity of $\boldsymbol{\omega}/2$.

The first term in (3.19) is the relative velocity between point P and point O caused by deformation of the fluid element defined by $d\mathbf{x}$. This deformation becomes particularly simple in a coordinate system coinciding with the principal axes of the strain-rate tensor. The components S_{ij} change as the coordinate system is rotated, and for one particular orientation of the coordinate system, a symmetric tensor has only diagonal components; these are called the *principal axes* of the tensor (see Section 2.12 and Example 2.4). Denoting the variables in this principal coordinate system by an over bar (Figure 3.13), the *first* part of (3.19) can be written as:

$$d\overline{\mathbf{u}} = \overline{\mathrm{S}} \cdot d\overline{\mathbf{x}} = \begin{bmatrix} \overline{S}_{11} & 0 & 0 \\ 0 & \overline{S}_{22} & 0 \\ 0 & 0 & \overline{S}_{33} \end{bmatrix} \begin{bmatrix} d\overline{x}_1 \\ d\overline{x}_2 \\ d\overline{x}_3 \end{bmatrix}. \tag{3.20}$$

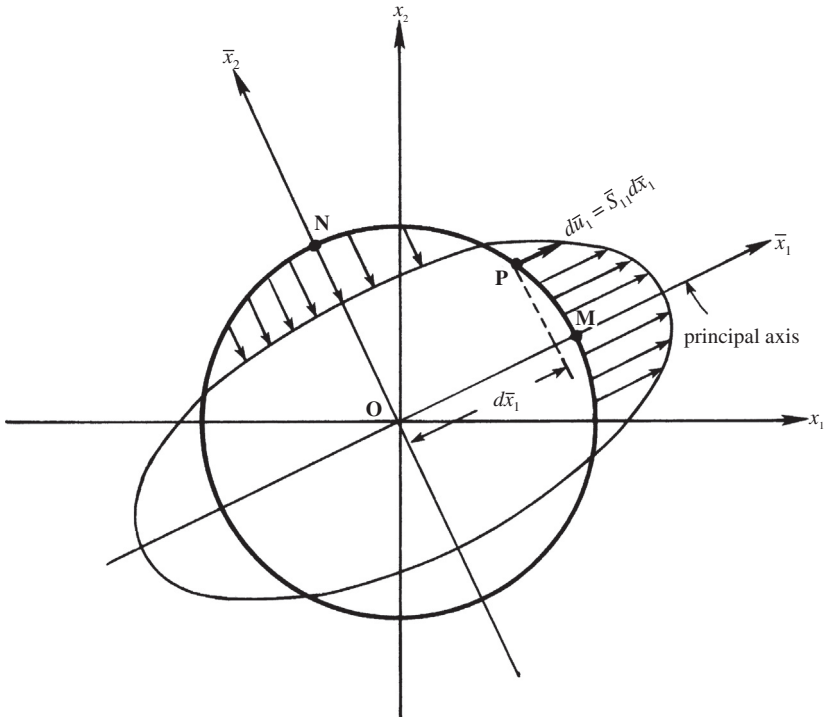

FIGURE 3.13 Deformation of a spherical fluid element into an ellipsoid. Here only the intersection of the element with the plane defined by the first and second coordinate directions is shown.

Here, $\overline{S}_{11}$, $\overline{S}_{22}$, and $\overline{S}_{33}$ are the diagonal components of $\mathbf{S}$ in the principal-axis coordinate system and are called the *eigenvalues* of $\mathbf{S}$. The three components of (3.20) can be written as

$$d\overline{u}_1 = \overline{S}_{11} d\overline{x}_1, \quad d\overline{u}_2 = \overline{S}_{22} d\overline{x}_2, \quad \text{and} \quad d\overline{u}_3 = \overline{S}_{33} d\overline{x}_3. \tag{3.21}$$

Consider the significance of $d\overline{u}_1 = \overline{S}_{11} d\overline{x}_1$ when $\overline{S}_{11}$ is positive. This equation implies that point P in Figure 3.9 is moving *away* from point O in the $\overline{x}_1$-direction at a rate proportional to the distance $d\overline{x}_1$. Considering all points on the surface of a sphere centered on O and having radius $|d\mathbf{x}|$ (see Figure 3.13), the movement of P in the $\overline{x}_1$ direction is maximum when P coincides with point M (where $d\overline{x}_1 = |d\mathbf{x}|$) and is zero when P coincides with point N (where $d\overline{x}_1 = 0$). Figure 3.13 illustrates the intersection of this sphere with the $(\overline{x}_1, \overline{x}_2)$-plane for the case where $\overline{S}_{11} > 0$ and $\overline{S}_{22} < 0$; the deformation in the x_3 direction is not shown in this figure. In a small interval of time, *a spherical fluid element around* O *therefore becomes an ellipsoid whose axes are the principal axes of the strain-rate tensor* $\mathbf{S}$.

Summary

The relative velocity in the neighborhood of a point can be divided into two parts. One part comes from rotation of the element, and the other part comes from deformation of the

element. A spherical element deforms to an ellipsoid whose axes coincide with the principal axes of the local strain-rate tensor.

3.5. KINEMATICS OF SIMPLE PLANE FLOWS

In this section, the rotation and deformation of fluid elements in two simple steady flows with straight and circular streamlines are considered in two-dimensional (x_1,x_2)-Cartesian and (r,θ)-polar coordinates, respectively. In both cases, the flows can be described with a single independent spatial coordinate that increases perpendicular to the flow direction.

First consider parallel shear flow where $\mathbf{u} = (u_1(x_2), 0)$ as shown in Figure 3.14. The lone nonzero velocity gradient is $\gamma(x_2) \equiv du_1/dx_2$, and, from (3.16), the only nonzero component of vorticity is $\omega_3 = -\gamma$. In Figure 3.14, the angular velocity of line element AB is $-\gamma$, and that of BC is zero, giving $-\gamma/2$ as the overall angular velocity (half the vorticity). The average value does not depend on *which* two mutually perpendicular elements in the (x_1,x_2)-plane are chosen to compute it.

In contrast, the components of the strain rate do depend on the orientation of the element. From (3.11), S_{ij} for a fluid element such as ABCD, with sides parallel to the x_1, x_2-axes, is

$$S_{ij} = \begin{bmatrix} 0 & \gamma/2 \\ \gamma/2 & 0 \end{bmatrix},$$

which shows that there are only off-diagonal elements of **S**. Therefore, the element ABCD undergoes shear, but no normal strain. As discussed in Section 2.11 and Example 2.4, a symmetric tensor with zero diagonal elements can be diagonalized by rotating the coordinate system through 45°. It is shown there that, along these *principal axes* (denoted by an overbar in Figure 3.14), the strain rate tensor is

$$\overline{S}_{ij} = \begin{bmatrix} \gamma/2 & 0 \\ 0 & -\gamma/2 \end{bmatrix},$$

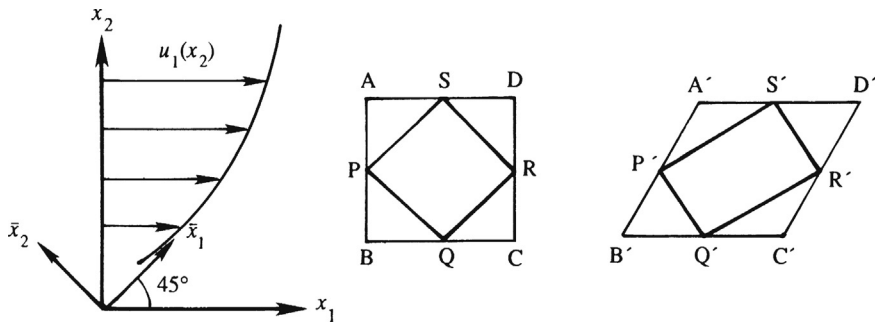

FIGURE 3.14 Deformation of elements in a parallel shear flow. The element is stretched along the principal axis $\bar{x}_1$ and compressed along the principal axis $\bar{x}_2$. The lengths of the sides of ADCB remain unchanged while the corner angles of SRQP remain unchanged.

so that along the first principle axis there is a linear extension rate of $\gamma/2$, along the second principle axis there is a linear compression rate of $-\gamma/2$, and there is no shear. This can be seen geometrically in Figure 3.14 by examining the deformation of an element PQRS oriented at 45°, which deforms to P′Q′R′S′. It is clear that the side PS elongates and the side PQ contracts, but the angles between the sides of the element remain at 90°. In a small time interval, a small spherical element in this flow would become an ellipsoid oriented at 45° to the x_1, x_2-coordinate system.

In summary, the element ABCD in a parallel shear flow deforms via shear without normal strain, whereas the element PQRS deforms via normal strain without shear strain. However, both elements rotate at the same angular velocity.

Now consider two steady vortex flows having circular streamlines. In (r,θ)-polar coordinates, both flows are defined by $u_r = 0$ and $u_\theta = u_\theta(r)$, with the first one being *solid-body rotation*,

$$u_r = 0 \quad \text{and} \quad u_\theta = \omega_0 r, \tag{3.22}$$

where ω_0 is a constant equal to the angular velocity of each particle about the origin (Figure 3.15). Such a flow can be generated by steadily rotating a cylindrical tank containing a viscous fluid about its axis and waiting until the transients die out. From Appendix B, the vorticity component in the z-direction perpendicular to the (r,θ)-plane is

$$\omega_z = \frac{1}{r}\frac{\partial}{\partial r}(ru_\theta) - \frac{1}{r}\frac{\partial u_r}{\partial \theta} = 2\omega_0, \tag{3.23}$$

which is independent of location. Thus, each fluid element is rotating about its own center at the same rate that it rotates about the origin of coordinates. This is evident in Figure 3.15, which shows the location of element ABCD at two successive times. The two mutually perpendicular fluid lines AD and AB both rotate counterclockwise (about the center of the

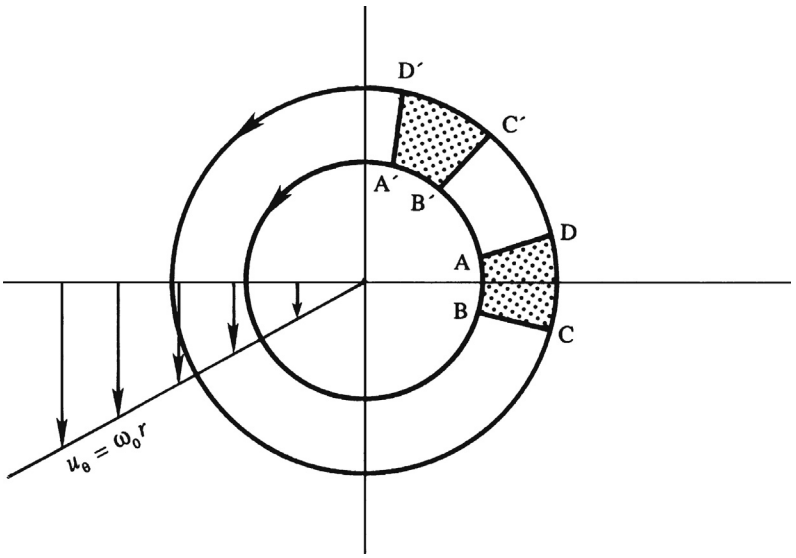

FIGURE 3.15 Solid-body rotation. The streamlines are circular and fluid elements spin about their own centers at the same rate that they revolve around the origin. There is no deformation of the elements, only rotation.

element) with speed ω_0. The time period for one *rotation* of the particle about its own center equals the time period for one *revolution* around the origin of coordinates. In addition, $\mathbf{S}=0$ for this flow so fluid elements do not deform and each retains its location relative to other elements, as is expected for solid-body rotation.

The circulation around a circuit of radius r in this flow is

$$\Gamma = \oint_C \mathbf{u}\cdot d\mathbf{s} = \int_0^{2\pi} u_\theta r d\theta = 2\pi r u_\theta = 2\pi r^2\omega_0, \tag{3.24}$$

which shows that circulation equals the vorticity, $2\omega_0$, times the area contained by C. This result is true for *any* circuit C, regardless of whether or not it contains the origin (see Exercise 3.23).

Another flow with circular streamlines is that from an ideal vortex line oriented perpendicular to the (r,θ)-plane. Here, the θ-component of fluid velocity is inversely proportional to the radius of the streamline and the radial velocity is again zero:

$$u_r = 0 \quad \text{and} \quad u_\theta = B/r, \tag{3.25}$$

where B is constant. From (3.23), the vorticity in this flow at any point away from the origin is $\omega_z=0$, but the circulation around a circuit of radius r centered on the origin is a nonzero constant,

$$\Gamma = \int_0^{2\pi} u_\theta r d\theta = 2\pi r u_\theta = 2\pi B, \tag{3.26}$$

independent of r. Thus, considering vorticity to be the circulation per unit area, as in (3.18) when $\mathbf{n}=\mathbf{e}_z$, then (3.26) implies that the flow specified by (3.25) is *irrotational everywhere except at $r=0$ where the vorticity is infinite with a finite area integral*:

$$[\omega_z]_{r\to 0} = \lim_{r\to 0}\frac{1}{A}\int_A \omega_z dA = \lim_{r\to 0}\frac{1}{\pi r^2}\oint_C \mathbf{u}\cdot d\mathbf{s} = \lim_{r\to 0}\frac{2B}{r^2}. \tag{3.27}$$

Although the circulation around a circuit containing the origin in an irrotational vortex flow is nonzero, that around a circuit *not* containing the origin is zero. The circulation around the contour ABCD (Figure 3.16) is

$$\Gamma_{\mathrm{ABCD}} = \left\{\int_{\mathrm{AB}} + \int_{\mathrm{BC}} + \int_{\mathrm{CD}} + \int_{\mathrm{DA}}\right\}\mathbf{u}\cdot d\mathbf{s}.$$

The line integrals of $\mathbf{u}\cdot d\mathbf{s}$ on BC and DA are zero because $\mathbf{u}$ and $d\mathbf{s}$ are perpendicular, and the remaining parts of the circuit ABCD produce

$$\Gamma_{\mathrm{ABCD}} = -[u_\theta r]_r \Delta\theta + [u_\theta r]_{r+\Delta r}\Delta\theta = 0,$$

where the line integral along AB is negative because $\mathbf{u}$ and $d\mathbf{s}$ are oppositely directed, and the final equality is obtained by noting that the product $u_\theta r = B$ is a constant. In addition, zero circulation around ABCD is expected because of Stokes' theorem and the fact that the vorticity vanishes everywhere within ABCD.

Real vortices, such as a bathtub vortex, a wing-tip vortex, or a tornado, do not mimic solid-body rotation over large regions of space, nor do they produce unbounded fluid velocity magnitudes near their axes of rotation. Instead, real vortices combine elements

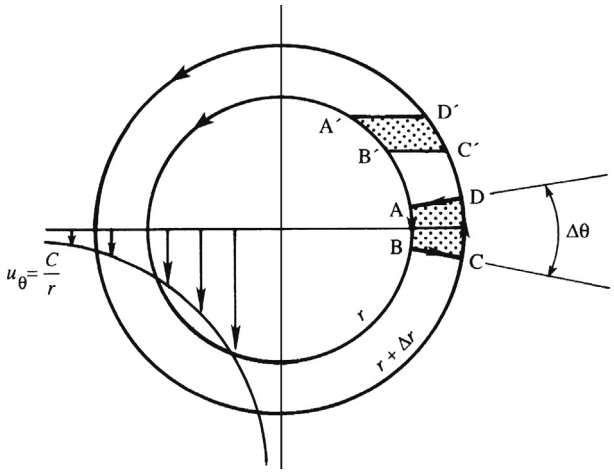

FIGURE 3.16 Irrotational vortex. The streamlines are circular, as for solid-body rotation, but the fluid velocity varies with distance from the origin so that fluid elements only deform; they do not spin. The vorticity of fluid elements is zero everywhere, except at the origin where it is infinite.

of the ideal vortex flows described by (3.22) and (3.25). Near the center of rotation, a real vortex's core flow is nearly solid-body rotation, but far from this core, real-vortex-induced flow is nearly irrotational. Two common idealizations of this behavior are the Rankine vortex defined by

$$\omega_z(r) = \begin{Bmatrix} \Gamma/\pi\sigma^2 = const. & \text{for } r \le \sigma \\ 0 & \text{for } r > \sigma \end{Bmatrix} \quad \text{and} \quad u_\theta(r) = \begin{Bmatrix} (\Gamma/2\pi\sigma^2)r & \text{for } r \le \sigma \\ \Gamma/2\pi r & \text{for } r > \sigma \end{Bmatrix}, \tag{3.28}$$

and the Gaussian vortex defined by

$$\omega_z(r) = \frac{\Gamma}{\pi\sigma^2}\exp\left(-r^2/\sigma^2\right) \quad \text{and} \quad u_\theta(r) = \frac{\Gamma}{2\pi r}\Big(1 - \exp\big(-r^2/\sigma^2\big)\Big). \tag{3.29}$$

In both cases, σ is a core-size parameter that determines the radial distance where real vortex behavior transitions from solid-body rotation to irrotational vortex flow. For the Rankine vortex, this transition is abrupt and occurs at $r = \sigma$ where u_θ reaches its maximum. For the Gaussian vortex, this transition is gradual and the maximum value of u_θ is reached at $r \approx 1.12091\sigma$ (see Exercise 3.26).

3.6. REYNOLDS TRANSPORT THEOREM

The final kinematic result needed for developing the differential and the control-volume versions of the conservation equations for fluid motion is the Reynolds transport theorem for time differentiation of integrals over arbitrarily moving and deforming volumes. Reynolds transport theorem is the three-dimensional extension of *Leibniz's theorem* for differentiating a single-variable integral having a time-dependent integrand and time-dependent limits (see Riley et al., 1998).

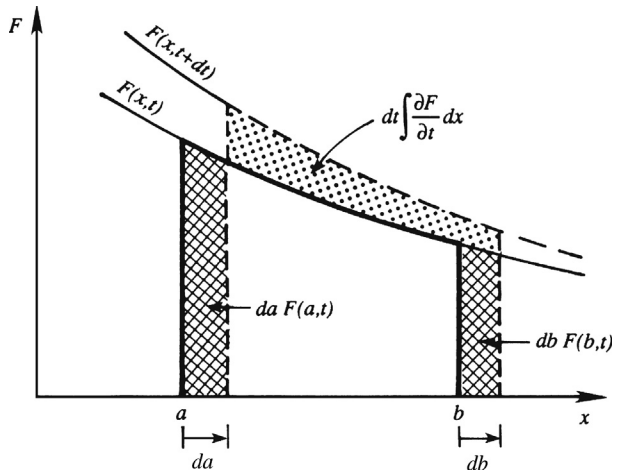

FIGURE 3.17 Graphical illustration of the Liebniz theorem. The three marked areas correspond to the three contributions shown on the right in (3.30). Here da, db, and $\partial F/\partial t$ are all shown as positive.

Consider a function F that depends on one independent spatial variable, x, and time t. In addition assume that the time derivative of its integral is of interest when the limits of integration, a and b, are themselves functions of time. Leibniz's theorem states the time derivative of the integral of $F(x,t)$ between $x=a(t)$ and $x=b(t)$ is

$$\frac{d}{dt}\int_{x=a(t)}^{x=b(t)} F(x,t)\,dx = \int_{a}^{b} \frac{\partial F}{\partial t}\,dx + \frac{db}{dt}F(b,t) - \frac{da}{dt}F(a,t), \tag{3.30}$$

where a, b, F, and their derivatives appearing on the right side of (3.30) are all evaluated at time t. This situation is depicted in Figure 3.17, where the three contributions are shown by dots and cross-hatches. The continuous line shows the integral $\int F dx$ at time t, and the dashed line shows the integral at time $t + dt$. The first term on the right side of (3.30) is the integral of $\partial F/\partial t$ between $x=a$ and b, the second term is the gain of F at the upper limit which is moving at rate db/dt, and the third term is the loss of F at the lower limit which is moving at rate da/dt. The essential features of (3.30) are the total time derivative on the left, an integral over the partial time derivative of the integrand on the right, and terms that account for the time-dependence of the limits of integration on the right. These features persist when (3.30) is generalized to three dimensions.

A largely geometrical development of this generalization is presented here using notation drawn from Thompson (1972). Consider a moving volume $V^*(t)$ having a (closed) surface $A^*(t)$ with outward normal $\mathbf{n}$ and let $\mathbf{b}$ denote the local velocity of A^* (Figure 3.18). The volume V^* and its surface A^* are commonly called a *control volume* and its *control surface*, respectively. The situation is quite general. The volume and its surface need not coincide with any particular boundary, interface, or surface. The velocity $\mathbf{b}$ need not be steady or uniform over $A^*(t)$. No specific coordinate system or origin of coordinates is needed. The goal of this effort is to determine the time derivative of the integral of a single-valued

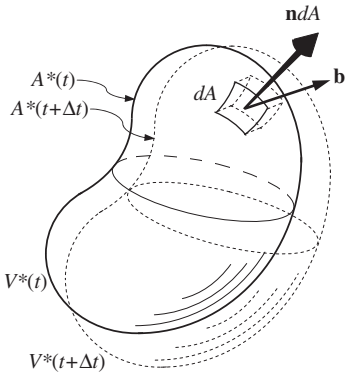

FIGURE 3.18 Geometrical depiction of a control volume $V^*(t)$ having a surface $A^*(t)$ that moves at a nonuniform velocity $\mathbf{b}$ during a small time increment Δt. When Δt is small enough, the volume increment $\Delta V = V^*(t+\Delta t) - V^*(t)$ will lie very near $A^*(t)$, so the volume-increment element adjacent to dA will be $(\mathbf{b}\Delta t) \cdot \mathbf{n}dA$ where $\mathbf{n}$ is the outward normal on $A^*(t)$.

continuous function $F(\mathbf{x}, t)$ in the volume $V^*(t)$. The starting point for this effort is the definition of a time derivative:

$$\frac{d}{dt}\int_{V^*(t)} F(\mathbf{x},t)dV = \lim_{\Delta t\to 0}\frac{1}{\Delta t}\left\{\int_{V^*(t+\Delta t)} F(\mathbf{x},t+\Delta t)dV - \int_{V^*(t)} F(\mathbf{x},t)dV\right\}. \tag{3.31}$$

The geometry for the two integrals inside the {,}-braces is shown in Figure 3.18 where solid lines are for time t while the dashed lines are for time $t+\Delta t$. The time derivative of the integral on the left is properly written as a total time derivative since the volume integration subsumes the possible spatial dependence of F. The first term inside the {,}-braces can be expanded to four terms by defining the volume increment $\Delta V \equiv V^*(t+\Delta t) - V^*(t)$ and Taylor expanding the integrand function $F(\mathbf{x}, t+\Delta t) \cong F(\mathbf{x}, t) + \Delta t(\partial F/\partial t)$ for $\Delta t \to 0$:

$$\begin{aligned}\int_{V^*(t+\Delta t)} F(\mathbf{x},t+\Delta t)dV \cong & \int_{V^*(t)} F(\mathbf{x},t)dV + \int_{V^*(t)} \Delta t\frac{\partial F(\mathbf{x},t)}{\partial t}\,dV + \int_{\Delta V} F(\mathbf{x},t)dV \\ & + \int_{\Delta V} \Delta t\frac{\partial F(\mathbf{x},t)}{\partial t}\,dV.\end{aligned} \tag{3.32}$$

The first term on the right in (3.32) will cancel with the final term in (3.31), and, when the limit in (3.31) is taken, both Δt and ΔV go to zero so the final term in (3.32) will not contribute because it is second order. Thus, when (3.32) is substituted into (3.31), the result is

$$\frac{d}{dt}\int_{V^*(t)} F(\mathbf{x},t)dV = \lim_{\Delta t\to 0}\frac{1}{\Delta t}\left\{\int_{V^*(t)} \Delta t\frac{\partial F(\mathbf{x},t)}{\partial t}\,dV + \int_{\Delta V} F(\mathbf{x},t)dV\right\}, \tag{3.33}$$

and this limit may be taken once the relationship between ΔV and Δt is known.

To find this relationship consider the motion of the small area element dA shown in Figure 3.18. In time Δt, dA sweeps out an elemental volume $(\mathbf{b}\Delta t) \cdot \mathbf{n} dA$ of the volume increment ΔV. Furthermore, this small element of ΔV is located adjacent to the surface $A^*(t)$. All these elemental contributions to ΔV may be summed together via a surface integral, and, as Δt goes to zero, the integrand value of $F(\mathbf{x},t)$ within these elemental volumes may be taken as that of F on the surface $A^*(t)$, thus

$$\int_{\Delta V} F(\mathbf{x},t) dV \cong \int_{A^*(t)} F(\mathbf{x},t)(\mathbf{b}\Delta t \cdot \mathbf{n}) dA \quad \text{as} \quad \Delta t \to 0. \tag{3.34}$$

Substituting (3.34) into (3.33), and taking the limit, produces the following statement of Reynolds transport theorem:

$$\frac{d}{dt}\int_{V^*(t)} F(\mathbf{x},t) dV = \int_{V^*(t)} \frac{\partial F(\mathbf{x},t)}{\partial t} dV + \int_{A^*(t)} F(\mathbf{x},t)\mathbf{b} \cdot \mathbf{n} dA. \tag{3.35}$$

This final result follows the pattern set by Liebniz's theorem that the total time derivative of an integral with time-dependent limits equals the integral of the partial time derivative of the integrand plus a term that accounts for the motion of the integration boundary. In (3.35), both inflows and outflows of F are accounted for through the dot product in the surface-integral term that monitors whether $A^*(t)$ is locally advancing ($\mathbf{b} \cdot \mathbf{n} > 0$) or retreating ($\mathbf{b} \cdot \mathbf{n} < 0$) along $\mathbf{n}$, so separate terms as in (3.30) are unnecessary. In addition, the $(\mathbf{x},t)$-space-time dependence of the control volume's surface velocity $\mathbf{b}$ and unit normal $\mathbf{n}$ are not explicitly shown in (3.35) because $\mathbf{b}$ and $\mathbf{n}$ are only defined on $A^*(t)$; neither is a field quantity like $F(\mathbf{x},t)$. Equation (3.35) is an entirely kinematic result, and it shows that d/dt may be moved inside a volume integral and replaced by $\partial/\partial t$ only when the integration volume, $V^*(t)$, is fixed in space so that $\mathbf{b} = 0$.

There are two physical interpretations of (3.35). The first, obtained when $F = 1$, is that volume is conserved as $V^*(t)$ moves through three-dimensional space, and under these conditions (3.35) is equivalent to (3.14) for small volumes (see Exercise 3.28). The second is that (3.35) is the extension of (3.5) to finite-size volumes (see Exercise 3.30). Nevertheless, (3.35) and judicious choices of F and $\mathbf{b}$ are the starting points in the next chapter for deriving the field equations of fluid motion from the principles of mass, momentum, and energy conservation.

EXAMPLE 3.2

The base radius r of a fixed-height right circular cone is increasing at the rate $\dot{r}$. Use Reynolds transport theorem to determine the rate at which the cone's volume is increasing when the cone's base radius is r_o if its height is h.

Solution

At any time, the volume V of the right circular cone is: $V = 1/3\ \pi h r^2$, which can be differentiated directly and evaluated at $r = r_o$ to find $dV/dt = 2/3\ \pi h r_o \dot{r}$. However, the task is to obtain this answer using (3.35). Choose V^* to perfectly enclose the cone so that $V^* = V$, and set $F = 1$ in (3.35) so that the time derivative of the cone's volume appears on the left:

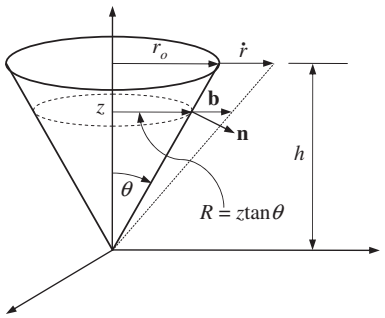

FIGURE 3.19 Conical geometry for Example 3.2. The cone's height is fixed but the radius of its circular surface (base) is increasing.

$$dV/dt = \int_{A^*(t)} \mathbf{b} \cdot \mathbf{n} dA.$$

Use the cylindrical coordinate system shown in Figure 3.19 with the cone's apex at the origin. Here, $\mathbf{b} = 0$ on the cone's base while $\mathbf{b} = (z/h)\dot{r}\mathbf{e}_R$ on its conical sides. The normal vector on the cone's sides is $\mathbf{n} = \mathbf{e}_R \cos\theta - \mathbf{e}_z \sin\theta$ where $r_o/h = \tan\theta$. Here, at the height z, the cone's surface area element is $dA = z\tan\theta d\varphi(dz/\cos\theta)$, where φ is the azimuthal angle, and the extra cosine factor enters because the conical surface is sloped. Thus, the volumetric rate of change becomes

$$\frac{dV}{dt} = \int_{z=0}^{h} \int_{\varphi=0}^{2\pi} \frac{z}{h} \dot{r}\mathbf{e}_R \cdot (\mathbf{e}_R \cos\theta - \mathbf{e}_z \sin\theta)\, z \tan\theta d\varphi \left(\frac{dz}{\cos\theta}\right)$$

$$= 2\pi \frac{\dot{r}\tan\theta}{h} \int_{z=0}^{h} z^2 dz = \frac{2}{3}\pi h^2 \dot{r}\tan\theta = \frac{2}{3}\pi h r_o \dot{r},$$

which recovers the answer obtained by direct differentiation.

EXERCISES

3.1. The gradient operator in Cartesian coordinates (x, y, z) is: $\nabla = \mathbf{e}_x(\partial/\partial x) + \mathbf{e}_y(\partial/\partial y) + \mathbf{e}_z(\partial/\partial z)$ where $\mathbf{e}_x$, $\mathbf{e}_y$, and $\mathbf{e}_z$ are the unit vectors. In cylindrical polar coordinates (R, φ, z) having the same origin (see Figure 3.3b), coordinates and unit vectors are related by: $R = \sqrt{x^2 + y^2}$, $\varphi = \tan^{-1}(y/x)$, and $z = z$; and $\mathbf{e}_R = \mathbf{e}_x \cos\varphi + \mathbf{e}_y \sin\varphi$, $\mathbf{e}_\varphi = -\mathbf{e}_x \sin\varphi + \mathbf{e}_y \cos\varphi$, and $\mathbf{e}_z = \mathbf{e}_z$. Determine the following in the cylindrical polar coordinate system.

a) $\partial\mathbf{e}_R/\partial\varphi$ and $\partial\mathbf{e}_\varphi/\partial\varphi$

b) the gradient operator ∇

c) the Laplacian operator $\nabla \cdot \nabla \equiv \nabla^2$

d) the divergence of the velocity field $\nabla \cdot \mathbf{u}$
e) the advective acceleration term $(\mathbf{u} \cdot \nabla)\mathbf{u}$
[See Appendix B for answers.]

3.2. Consider Cartesian coordinates (as given in Exercise 3.1) and spherical polar coordinates (r, θ, φ) having the same origin (see Figure 3.3c). Here coordinates and unit vectors are related by: $r = \sqrt{x^2 + y^2 + z^2}$, $\theta = \tan^{-1}(\sqrt{x^2 + y^2}/z)$, and $\varphi = \tan^{-1}(y/x)$; and $\mathbf{e}_r = \mathbf{e}_x \cos\varphi\sin\theta + \mathbf{e}_y \sin\varphi\sin\theta + \mathbf{e}_z \cos\theta$, $\mathbf{e}_\theta = \mathbf{e}_x \cos\varphi\cos\theta + \mathbf{e}_y \sin\varphi\cos\theta - \mathbf{e}_z \sin\theta$, and $\mathbf{e}_\varphi = -\mathbf{e}_x \sin\varphi + \mathbf{e}_y \cos\varphi$. In the spherical polar coordinate system, determine the following items.
a) $\partial\mathbf{e}_r/\partial\theta$, $\partial\mathbf{e}_r/\partial\varphi$, $\partial\mathbf{e}_\theta/\partial\theta$, $\partial\mathbf{e}_\theta/\partial\varphi$, and $\partial\mathbf{e}_\varphi/\partial\varphi$
b) the gradient operator ∇
c) the Laplacian $\nabla \cdot \nabla \equiv \nabla^2$
d) the divergence of the velocity field $\nabla \cdot \mathbf{u}$
e) the advective acceleration term $(\mathbf{u} \cdot \nabla)\mathbf{u}$
[See Appendix B for answers.]

3.3. If $d\mathbf{s} = (dx, dy, dz)$ is an element of arc length along a streamline (Figure 3.5) and $\mathbf{u} = (u, v, w)$ is the local fluid velocity vector, show that if $d\mathbf{s}$ is everywhere tangent to $\mathbf{u}$ then $dx/u = dy/v = dz/w$.

3.4. For the two-dimensional steady flow having velocity components $u = Sy$ and $v = Sx$, determine the following when S is a positive real constant having units of inverse time.
a) equations for the streamlines with a sketch of the flow pattern
b) the components of the strain-rate tensor
c) the components of the rotation tensor
d) the coordinate rotation that diagonalizes the strain-rate tensor, and the principal strain rates

3.5. Repeat Exercise 3.4 when $u = -Sx$ and $v = +Sy$. How are the two flows related?

3.6. At the instant shown in Figure 3.2b, the (u,v)-velocity field in Cartesian coordinates is $u = A(y^2 - x^2)/(x^2 + y^2)^2$, and $v = -2Axy/(x^2 + y^2)^2$ where A is a positive constant. Determine the equations for the streamlines by rearranging the first equality in (3.7) to read $udy - vdx = 0 = (\partial\psi/\partial y)dy + (\partial\psi/\partial x)dx$ and then looking for a solution in the form $\psi(x, y) = const$.

3.7. Determine the equivalent of the first equality in (3.7) for two-dimensional (r,θ)-polar coordinates, and then find the equation for the streamline that passes through (r_o, θ_o) when $\mathbf{u} = (u_r, u_\theta) = (A/r, B/r)$ where A and B are constants.

3.8. Determine the streamline, path line, and streak line that pass through the origin of coordinates at $t = t'$ when $u = U_o + \omega\xi_o\cos(\omega t)$ and $v = \omega\xi_o\sin(\omega t)$ in two-dimensional Cartesian coordinates where U_o is a constant horizontal velocity. Compare your results to those in Example 3.1 for $U_o \to 0$.

3.9. Compute and compare the streamline, path line, and streak line that pass through (1,1,0) at $t = 0$ for the following Cartesian velocity field $\mathbf{u} = (x, -yt, 0)$.

3.10. Consider a time-dependent flow field in two-dimensional Cartesian coordinates where $u = \ell\tau/t^2$, $v = xy/\ell\tau$, and ℓ and τ are constant length and time scales, respectively.
a) Use dimensional analysis to determine the functional form of the streamline through $\mathbf{x}'$ at time t'.

b) Find the equation for the streamline through $\mathbf{x}'$ at time t' and put your answer in dimensionless form.
c) Repeat part b) for the path line through $\mathbf{x}'$ at time t'.
d) Repeat part b) for the streak line through $\mathbf{x}'$ at time t'.

3.11. The velocity components in an unsteady plane flow are given by $u = x/(1+t)$ and $v = 2y/(2+t)$. Determine equations for the streamlines and path lines subject to $\mathbf{x} = \mathbf{x}_0$ at $t = 0$.

3.12. Using the geometry and notation of Figure 3.8, prove (3.9).

3.13. Determine the unsteady, $\partial\mathbf{u}/\partial t$, and advective, $(\mathbf{u}\cdot\nabla)\mathbf{u}$, fluid acceleration terms for the following flow fields specified in Cartesian coordinates.
a) $\mathbf{u} = (u(y,z,t), 0, 0)$
b) $\mathbf{u} = \Omega \times \mathbf{x}$ where $\Omega = (0, 0, \Omega_z(t))$
c) $\mathbf{u} = A(t)(x, -y, 0)$
d) $\mathbf{u} = (U_o + u_o \sin(kx - \Omega t), 0, 0)$ where U_o, u_o, k, and Ω are positive constants

3.14. Consider the following Cartesian velocity field $\mathbf{u} = A(t)(f(x), g(y), h(z))$ where A, f, g, and h are nonconstant functions of only one independent variable.
a) Determine $\partial\mathbf{u}/\partial t$ and $(\mathbf{u}\cdot\nabla)\mathbf{u}$ in terms of A, f, g, and h, and their derivatives.
b) Determine A, f, g, and h when $D\mathbf{u}/Dt = 0$, $\mathbf{u} = 0$ at $\mathbf{x} = 0$, and $\mathbf{u}$ is finite for $t > 0$.
c) For the conditions in part b), determine the equation for the path line that passes through $\mathbf{x}_o$ at time t_o, and show directly that the acceleration $\mathbf{a}$ of the fluid particle that follows this path is zero.

3.15. If a velocity field is given by $u = ay$ and $v = 0$, compute the circulation around a circle of radius r_o that is centered on the origin. Check the result by using Stokes' theorem.

3.16. Consider a plane Couette flow of a viscous fluid confined between two flat plates a distance b apart. At steady state the velocity distribution is $u = Uy/b$ and $v = w = 0$, where the upper plate at $y = b$ is moving parallel to itself at speed U, and the lower plate is held stationary. Find the rates of linear strain, the rate of shear strain, and vorticity in this flow.

3.17. For the flow field $\mathbf{u} = \mathbf{U} + \boldsymbol{\Omega} \times \mathbf{x}$, where $\mathbf{U}$ and $\boldsymbol{\Omega}$ are constant linear- and angular-velocity vectors, use Cartesian coordinates to a) show that S_{ij} is zero, and b) determine R_{ij}.

3.18. Starting with a small rectangular volume element $\delta V = \delta x_1 \delta x_2 \delta x_3$, prove (3.14).

3.19. Let $Oxyz$ be a stationary frame of reference, and let the z-axis be parallel with fluid vorticity vector in the vicinity of O so that $\boldsymbol{\omega} = \nabla \times \mathbf{u} = \omega_z \mathbf{e}_z$ in this frame of reference. Now consider a second rotating frame of reference $Ox'y'z'$ having the same origin that rotates about the z-axis at angular rate $\Omega\mathbf{e}_z$. Starting from the kinematic relationship, $\mathbf{u} = (\Omega\mathbf{e}_z) \times \mathbf{x} + \mathbf{u}'$, show that in the vicinity of O the vorticity $\boldsymbol{\omega}' = \nabla' \times \mathbf{u}'$ in the rotating frame of reference can only be zero when $2\Omega = \omega_z$, where ∇' is the gradient operator in the primed coordinates. The following unit vector transformation rules may be of use: $\mathbf{e}'_x = \mathbf{e}_x \cos(\Omega t) + \mathbf{e}_y \sin(\Omega t)$, $\mathbf{e}'_y = -\mathbf{e}_x \sin(\Omega t) + \mathbf{e}_y \cos(\Omega t)$, and $\mathbf{e}'_z = \mathbf{e}_z$.

3.20. Consider a plane-polar area element having dimensions dr and $rd\theta$. For two-dimensional flow in this plane, evaluate the right-hand side of Stokes' theorem

$\int \boldsymbol{\omega} \cdot \mathbf{n} dA = \int \mathbf{u} \cdot d\mathbf{s}$ and thereby show that the expression for vorticity in plane-polar coordinates is: $\omega_z = \frac{1}{r}\frac{\partial}{\partial r}(ru_\theta) - \frac{1}{r}\frac{\partial u_r}{\partial \theta}$.

3.21. The velocity field of a certain flow is given by $u = 2xy^2 + 2xz^2$, $v = x^2y$, and $w = x^2z$. Consider the fluid region inside a spherical volume $x^2 + y^2 + z^2 = a^2$. Verify the validity of Gauss' theorem $\iiint_V \nabla \cdot \mathbf{u} dV = \iint_A \mathbf{u} \cdot \mathbf{n} dA$ by integrating over the sphere.

3.22. A flow field on the xy-plane has the velocity components $u = 3x + y$ and $v = 2x - 3y$. Show that the circulation around the circle $(x-1)^2 + (y-6)^2 = 4$ is 4π.

3.23. Consider solid-body rotation about the origin in two dimensions: $u_r = 0$ and $u_\theta = \omega_0 r$. Use a polar-coordinate element of dimension $rd\theta$ and dr, and verify that the circulation is vorticity times area. (In Section 3.5 this was verified for a circular element surrounding the origin.)

3.24. Consider the following steady Cartesian velocity field $\mathbf{u} = \left(\frac{-Ay}{(x^2+y^2)^\beta}, \frac{+Ax}{(x^2+y^2)^\beta}, 0\right)$.

- **a)** Determine the streamline that passes through $\mathbf{x} = (x_o, y_o, 0)$.
- **b)** Compute R_{ij} for this velocity field.
- **c)** For $A > 0$, explain the sense of rotation (i.e., clockwise or counterclockwise) for fluid elements for $\beta < 1$, $\beta = 1$, and $\beta > 1$.

3.25. Using indicial notation (and no vector identities), show that the acceleration $\mathbf{a}$ of a fluid particle is given by $\mathbf{a} = \partial \mathbf{u}/\partial t + \nabla\left(\frac{1}{2}|\mathbf{u}|^2\right) + \boldsymbol{\omega} \times \mathbf{u}$, where $\boldsymbol{\omega}$ is the vorticity.

3.26. Starting from (3.29), show that the maximum u_θ in a Gaussian vortex occurs when $1 + 2(r^2/\sigma^2) = \exp(r^2/\sigma^2)$. Verify that this implies $r \approx 1.12091\sigma$.

3.27. [1]For the following time-dependent volumes $V^*(t)$ and smooth single-valued integrand functions F, choose an appropriate coordinate system and show that $(d/dt)\int_{V^*(t)} F dV$ obtained from (3.30) is equal to that obtained from (3.35).

- **a)** $V^*(t) = L_1(t)L_2L_3$ is a rectangular solid defined by $0 \le x_i \le L_i$, where L_1 depends on time while L_2 and L_3 are constants, and the integrand function $F(x_1,t)$ depends only on the first coordinate and time.
- **b)** $V^*(t) = (\pi/4)d^2(t)L$ is a cylinder defined by $0 \le R \le d(t)/2$ and $0 \le z \le L$, where the cylinder's diameter d depends on time while its length L is constant, and the integrand function $F(R,t)$ depends only on the distance from the cylinder's axis and time.
- **c)** $V^*(t) = (\pi/6)D^3(t)$ is a sphere defined by $0 \le r \le D(t)/2$ where the sphere's diameter D depends on time, and the integrand function $F(r,t)$ depends only on the radial distance from the center of the sphere and time.

3.28. Starting from (3.35), set $F = 1$ and derive (3.14) when $\mathbf{b} = \mathbf{u}$ and $V^*(t) = \delta V \to 0$.

3.29. For a smooth, single-valued function $F(\mathbf{x})$ that only depends on space and an arbitrarily shaped control volume that moves with velocity $\mathbf{b}(t)$ that only depends on time, show that $(d/dt)\int_{V^*(t)} F(\mathbf{x}) dV = \mathbf{b} \cdot (\int_{V^*(t)} \nabla F(\mathbf{x}) dV)$.

3.30. Show that (3.35) reduces to (3.5) when $V^*(t) = \delta V \to 0$ and the control surface velocity $\mathbf{b}$ is equal to the fluid velocity $\mathbf{u}(\mathbf{x},t)$.

[1]Developed from Problem 1.9 on page 48 in Thompson (1972)

Literature Cited

Meriam, J. L., and Kraige, L. G. (2007). *Engineering Mechanics, Dynamics* (6th ed). Hoboken, NJ: John Wiley and Sons, Inc.

Raffel, M., Willert, C., and Kompenhans, J. (1998). *Particle Image Velocimetry.* Berlin: Springer.

Riley, K. F., Hobson, M. P., and Bence, S. J. (1998). *Mathematical Methods for Physics and Engineering* (3rd ed.). Cambridge, UK: Cambridge University Press.

Samimy, M., Breuer, K. S., Leal, L. G., and Steen, P. H. (2003). *A Gallery of Fluid Motion*. Cambridge, UK: Cambridge University Press.

Thompson, P. A. (1972). *Compressible-Fluid Dynamics*. New York: McGraw-Hill.

Van Dyke, M. (1982). *An Album of Fluid Motion*. Stanford, California: Parabolic Press.

Supplemental Reading

Aris, R. (1962). *Vectors, Tensors, and the Basic Equations of Fluid Mechanics.* Englewood Cliffs, NJ: Prentice-Hall. (The distinctions among streamlines, path lines, and streak lines in unsteady flows are explained, with examples.)

Prandtl, L., and Tietjens, O. C. (1934). *Fundamentals of Hydro- and Aeromechanics*. New York: Dover Publications. (Chapter V contains a simple but useful treatment of kinematics.)

Prandtl, L., and Tietjens, O. G. (1934). *Applied Hydro- and Aeromechanics*. New York: Dover Publications. (This volume contains classic photographs from Prandtl's laboratory.)